Electric Power Components and Systems 11 H 44 14 11 Power-system Stability Improvement by PSO Optimized SSSC-based Damping Controller Abstract Power-system stability improvement by a static synchronous series com-pensator (SSSC)-based damping controller is thoroughly investigated in this article. The design problem of the proposed controller is	Các linh kiện và hệ thống điện Cải thiện độ ổn định của hệ thống điện bằng bộ điều khiển SSSC tối ưu PSO Tóm tắt Trong bài báo này, chúng ta sẽ phân tích một cách thấu đáo phương pháp cải thiện độ ổn định hệ thống điện bằng bộ điều khiển tắt dần hoạt động dựa trên thiết bị bù tĩnh (SSSC). Bài toán thiết kế bộ điều

formulated as an optimization problem, and the particle swarm optimization technique is employed to search for the optimal controller parameters. By minimizing a time-domain-based objective function, in which the deviation in the oscillatory rotor speed of the generator is involved, stability performance of the system is improved. The performance of the proposed controller is evaluated under different disturbances for both a single-machine infinite- bus power system and a multi-machine power system. Results are presented to show the effectiveness of the proposed controller. It is observed that the proposed SSSC- based controller provides efficient damping to power-system oscillations and greatly improves the system voltage profile under various severe disturbances. Furthermore, the simulation results show that in a multi-machine power system, the modal oscilla-tions are effectively damped by the proposed SSSC controller.

1. Introduction

When large power systems are interconnected by relatively weak tie lines, low-frequency oscillations are observed. These oscillations may sustain and grow to cause system sepa-ration if no adequate damping is available [1]. Recent development of power electronics introduces the use of flexible AC transmission system (FACTS) controllers in power systems. FACTS controllers are capable of controlling the network condition in a very fast manner, and this feature of FACTS can be exploited to improve the stability of a power system [2]. The static

khiển đề xuất được phát biểu dưới dạng bài toán tối ưu hóa, và kỹ thuật tối ưu hóa bầy đàn (tối ưu quần thể) được sử dụng để tìm các tham số tối ưu cho bộ điều khiển. Bằng cách làm cho hàm mục tiêu miền thời gian đạt giá trị cực tiểu, trong đó có chứa độ lệch tốc độ rotor dao động của máy phát, sự ổn định của hệ thống được cải thiện. Hiệu suất của bộ điều khiển do chúng tôi đề xuất được đánh giá trong những điều kiện nhiễu khác nhau đối với cả hệ thống điện lưới vô cùng lớn một nguồn và hệ thống điện nhiều nguồn. Các kết quả được trình bày cho thấy hiệu quả của bộ điều khiển được đề xuất. Chúng ta thấy rằng bộ điều khiển SSSC đề xuất làm suy giảm có hiệu quả các dao động của hệ thống điện và cải thiện đáng kể dạng điện áp hệ thống trong các điều kiện nhiễu khắc nghiệt (nghiêm trọng) khác nhau. Hơn nữa, các kết quả mô phỏng cho thấy rằng trong hệ thống điện nhiều nguồn, các mode dao động bị làm giảm một cách hiệu quả nhờ vào bộ điều khiển SSSC đề xuất.

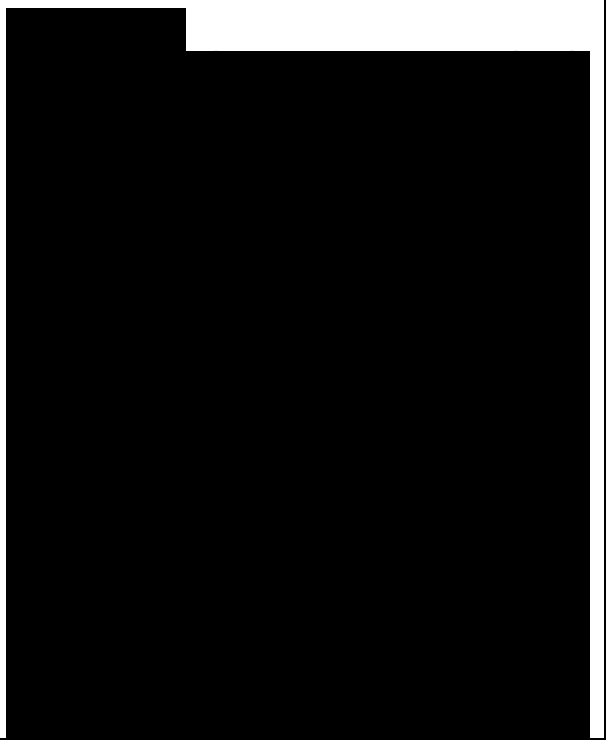

synchronous series compensator (SSSC) is one of the important members of a FACTS family that can be installed in series in the transmission lines. The SSSC is very effective in controlling power flow in a transmission line with the capability to change its reactance characteristic from capacitive to inductive [3]. An auxiliary stabilizing signal can also be superimposed on the power flow control function of the SSSC so as to improve power-system stability [4]. In the case of a singlemachine infinite-bus power system (i.e., the situations where a generator is connected to a large system), the use of the power-system stabilizer (PSS) can have satisfactory results in damping the power-system oscillations. Therefore, in such a situation, the PSS is more preferable than an SSSC, which is more expensive and difficult to control. But in the multi-machine power system, the use of the PSS needs a precise study and sometimes may reduce the system stability if not well tuned. Also, PSSs are effective in damping only local modes of oscillations. Therefore, in the present study, an SSSC has been considered, and its effectiveness in damping both inter-area and local mode of oscillations has been analyzed. The application of an SSSC for power oscillation damping, stability enhancement, and frequency stabilization can be found in several references [5-8]. The influence of degree of compensation and mode of operation of an SSSC on small disturbance and transient stability is also reported in the literature [9-11]. Most of these proposals are based on

small disturbance analysis that requires linearization of the system involved. However, linear methods cannot properly capture complex dynamics of the system, especially during major disturbances. This presents difficulties for tuning the FACTS controllers in that the controllers tuned to provide desired performance at small signal conditions do not guarantee acceptable performance in the event of major disturbances. Also, the performance of the controller under unbalanced faults cannot be evaluated by using the linear single-phase models. In order to overcome the above shortcomings, this study uses three-phase models of SSSC and power-system components.

A conventional lead-lag controller structure is preferred by the power-system utilities because of the ease of on-line tuning and also lack of assurance of the stability by some adaptive or variable structure techniques. A number of conventional techniques have been reported in the literature pertaining to design problems of conventional PSSs, namely the eigenvalue assignment, mathematical programming, gradient procedure for optimization, and also the modern control theory. Unfortunately, the conventional techniques are time consuming as they are iterative and require heavy computation burden and slow convergence. In addition, the search process is susceptible to be trapped in local minima, and the solution obtained may not be optimal [12].

Recently, the particle swarm optimization (PSO) technique appeared as a promising algorithm for

handling the optimization problems. PSO is a population-based stochastic optimization technique, inspired by social behavior of bird flocking or fish schooling [13]. PSO shares many similarities with the genetic algorithm (GA), such as initialization of population of random solutions and search for the optimal by updating generations. However, unlike GA, PSO has no evolution operators, such as crossover and mutation. One of the most promising advantages of PSO over the GA is its algorithmic simplicity— it uses a few parameters and is easy to implement. Therefore, PSS is employed in the present work to optimally tune the parameters of the SSSC-based damping controller.

In this article, a comprehensive assessment of the effects of the SSSC-based damping controller has been carried out. The design problem of the SSSC-based controller to improve power-system stability is transformed into an optimization problem. A PSO-based optimal tuning algorithm is used to optimally tune the parameters of the SSSC- based damping controller. The proposed controller has been applied and tested under different disturbances for a weakly connected single-machine infinite-bus and a multimachine power system. Simulation results are presented at different operating conditions and under various disturbances to show the effectiveness of the proposed controller. The sample power systems studied in this article are simple two-area examples with an SSSC. By studying simple systems, the basic characteristics of the controller can be

assessed and analyzed, and conclusions can be drawn to give an insight for larger systems with an SSSC. Furthermore, since all of the essential dynamics required for the power-system stability studies have been included, and the results have been obtained using three-phase models, general conclusions can be drawn from the results presented in the article so as to implement an SSSC in a large realistic power system.

2. System Model

2.1. Single-machine Infinite-bus Power System with SSSC

To design and optimize the SSSC-based damping controller, a single-machine infinite- bus system with SSSC, shown in Figure 1, is considered at the first instance. The system comprises a synchronous generator connected to an infinite bus through a step-up transformer and an SSSC followed by a double-circuit transmission line. The generator is represented by a sixth-order model and is equipped with a hydraulic turbine and governor (HTG) and excitation system. The HTG represents a non-linear hydraulic turbine model, a proportional integral derivative (PID) governor system, and a servomotor. The excitation system consists of a voltage regulator and DC exciter, without the exciter's saturation function [14]. In Figure 1, T/F represents the transformer; VS and VR are the generator terminal and infinite-bus voltages, respectively; V1 and V2 are the bus voltages; VDC and Vcnv are the DC voltage source and output voltage of the SSSC converter, respectively; I is the line current; and PL and PL1 are the total real power

flow in the transmission lines and that in one line, respectively. All of the relevant parameters are given in Appendix A.

2.2. Overview of the SSSC and Its Control System

An SSSC is a solid-state voltage-sourced converter (VSC), which generates a controllable AC voltage source and is connected in series to power transmission lines in a power system. The injected voltage (Vq) is in quadrature with the line current, I, and emulates an inductive or a capacitive reactance so as to influence the power flow in the transmission lines [3]. The compensation level can be controlled dynamically by changing the magnitude and polarity of Vq and the device can be operated both in capacitive and inductive mode.

The single-line block diagram of the control system of the SSSC is shown in Figure 2 [14] . In the control system block diagram, Vdcnv and Vqcnv designate the components of converter voltage Vcnv, which are, respectively, in phase and in quadrature with line current I. The control system consists of:

Figure 1. Single-machine infinite-bus power system with an SSSC.

Figure 2. Single-line diagram of the SSSC control system.

- a phase-locked loop (PLL) that synchronizes on the positive-sequence component of current I, the output of which is used to compute the direct-axis and quadrature- axis components of the AC three-phase voltages and currents;
- measurement systems that measure the q components of the AC

positive-sequence of voltages V and V2 (V\q and V2q) and the DC voltage VDC; and

- AC and DC voltage regulators that compute the two components of the converter voltage (Vdcnv and Vqcnv) that is required to obtain the desired DC voltage (Vdcref) and the injected voltage (Vqref).

The variation of injected voltage is performed by means of a VSC that is connected on the secondary side of a coupling transformer. The VSC uses forced-commutated power electronic devices (e.g., gate turn-off (GTO), integrated gate bipolar transistors (IGBT), or integrated gate-commutated thyristors (IGCT)) to synthesize a voltage Vcnv from a DC voltage source. A capacitor connected on the DC side of the VSC acts as a DC voltage source. A small active power is drawn from the line to keep the capacitor charged and to provide transformer and VSC losses, so that the injected voltage is practically 90° out of phase with current I.

Two types of technologies can be used for the VSC:

- VSC using GTO-based square-wave inverters and special interconnection trans-formers. Typically, four three-level inverters are used to build a 48-step voltage waveform. Special interconnection transformers are used to neutralize harmonics contained in the square waves that are generated by individual inverters. In this type of VSC, the fundamental component of voltage Vcnv is proportional to the voltage VDC. Therefore, VDC has to be varied for controlling the injected voltage.

• VSC using IGBT-based pulse-width-modulation (PWM) inverters. This type of inverter uses a PWM technique to synthesize a sinusoidal waveform from a DC voltage with a typical chopping frequency of a few kHz. Harmonics are cancelled by connecting filters at the AC side of the VSC. This type of VSC uses a fixed DC voltage VDC. Voltage Vcnv is varied by changing the modulation index of the PWM modulator.

A VSC using IGBT-based PWM inverters is used in the present study. However, as details of the inverter and harmonics are not represented in power-system stability studies, the same model can be used to represent a GTO-based model. A brief introduction about three-level GTO-based converters and PWM converters is given in Appendix B.

3. The Proposed Approach

3.1. Structure of the SSSC-based Damping Controller

The structure of the SSSC-based damping controller, to modulate the SSSC-injected voltage, Vq, is shown in Figure 3. The input signal of the proposed controller is the speed deviation (A!), and the output signal is the injected voltage Vq. The structure consists of a gain block with gain KS, a signal washout block, and a two-stage phase compensation block as shown in Figure 3. The signal washout block serves as a high-pass filter, with the time constant TW, that is high enough to allow signals associated with the oscillations in input signal to pass unchanged. From the viewpoint of the washout function, the value of TW is not critical and may be in the range of 1 to 20 sec [1]. The phase

compensation blocks (time constants T\S, T2S, T3S, and T4S) provide the appropriate phase-lead characteristics to compensate for the phase lag between the input and output signals. In Figure 3, Vqref represents the reference-injected voltage as desired by the steady-state power flow control loop. The steady-state power flow loop acts quite slowly in practice, and hence, in the present study, Vqref is assumed to be constant during large disturbance transient periods. The desired value of compensation is obtained according to the change in the SSSC-injected voltage AVq, which is added to Vqref.

3.2. Problem Formulation

The transfer function of the SSSC-based controller is

where USSSC and y are the output and input signals of the SSSC-based controller, respectively.

In the lead-lag structured controllers, the washout time constants, TW, and the denominator time constants, T2S and T4S, are usually prespecified [12, 15]. In the present study, TW = 10 sec and T2S = T4S = 0.3 sec are used. The controller gain, KS, and the time constants, T\S and T3S, are to be determined. During steady-state conditions, AVq and Vqref are constant. During dynamic conditions, the series injected voltage, Vq, is modulated to damp system oscillations. The effective Vq in dynamic conditions is given by

$$Vq = Vqref + A\,Vq\,. \qquad (2)$$

3.3. Optimization Problem

It is worth mentioning that the SSSC-based controller is designed to minimize the power- system oscillations after a large disturbance so

as to improve the power-system stability. These oscillations are reflected in the deviations in power angle, rotor speed, and tie-line power. Minimization of any one, or all, of the above deviations could be chosen as the objective. In the present study, an integral time absolute error of the speed deviations is taken as the objective function for single-machine infinite-bus power system. For the case of multi-machine power system, an integral time absolute error of the speed signals corresponding to the local and inter-area modes of oscillations is taken as the objective function. The objective functions are expressed as:

For a single-machine infinite-bus power system:

P t =tsim

J = I | A! • t • dt. (3)

For a multi-machine power system:

(4)

where Aw is the speed deviation in the single-machine infinite-bus system; AwL and A!/ are the speed deviations of inter-area and local modes of oscillations, respectively; and tsim is the time range of the simulation. With the variation of the SSSC-based damping controller parameters, these speed deviations will also be changed. For objective function calculation, the time-domain simulation of the power-system model is carried out for the simulation period. It is aimed to minimize this objective function in order to improve the system response in terms of the settling time and overshoots. The problem constraints are the SSSC controller parameter bounds. Therefore, the design problem can be formulated as the following

optimization problem:

(5)

subject to K!?in < Ks < K?”

T1S < T1S < T1S ,

(6)

Tuning a controller parameter can be viewed as an optimization problem in multi-modal space, as many settings of the controller could be yielding good performance. The traditional method of tuning does not guarantee optimal parameters, and in most cases, the tuned parameter needs improvement through trial and error. In the PSO-based method, the tuning process is associated with an optimality concept through the defined objective function and the time domain simulation. The designer has the freedom to explicitly specify the required performance objectives in terms of time domain bounds on the closed-loop responses. Hence, the PSO methods yield optimal parameters, and the method is free from the curse of local optimality. In view of the above, the proposed approach employs PSO to solve this optimization problem and search for an optimal set of SSSC-based damping controller parameters.

4. Overview of the PSO Technique

The PSO method is a member of wide a category of swarm intelligence methods for solving optimization problems. It is a population-based search algorithm, where each individual is referred to as a particle and represents a candidate solution. Each particle in PSO flies through the search space with an adaptable velocity that is dynamically modified according to its own flying experience and also to the flying experience of the

other particles. In PSO, particles strive to improve themselves by imitating traits from their successful peers. Furthermore, each particle has a memory, and hence, it is capable of remembering the best position in the search space that it ever visited. The position corresponding to the best fitness is known as pbest, and the overall best out of all the particles in the population is called gbest [16].

The features of the searching procedure can be summarized as follows [17].

- Initial positions of pbest and gbest are different. However, using the different directions of pbest and gbest, all agents gradually get close to the global optimum.
- The modified value of the agent position is continuous, and the method can be applied to the continuous problem. However, the method can be applied to the discrete problem using grids for the XY position and its velocity.
- There are no inconsistencies in searching procedures, even if continuous and discrete state variables are utilized with continuous axes and grids for XY posi-tions and velocities. Namely, the method can be naturally and easily applied to mixed-integer non-linear optimization problems with continuous and discrete state variables.

The modified velocity and position of each particle can be calculated using the current velocity and the distance from the pbest jg to gbestg, as shown in the following equations [18]:

where

n = number of particles in a swarm; m = number of components in a particle;

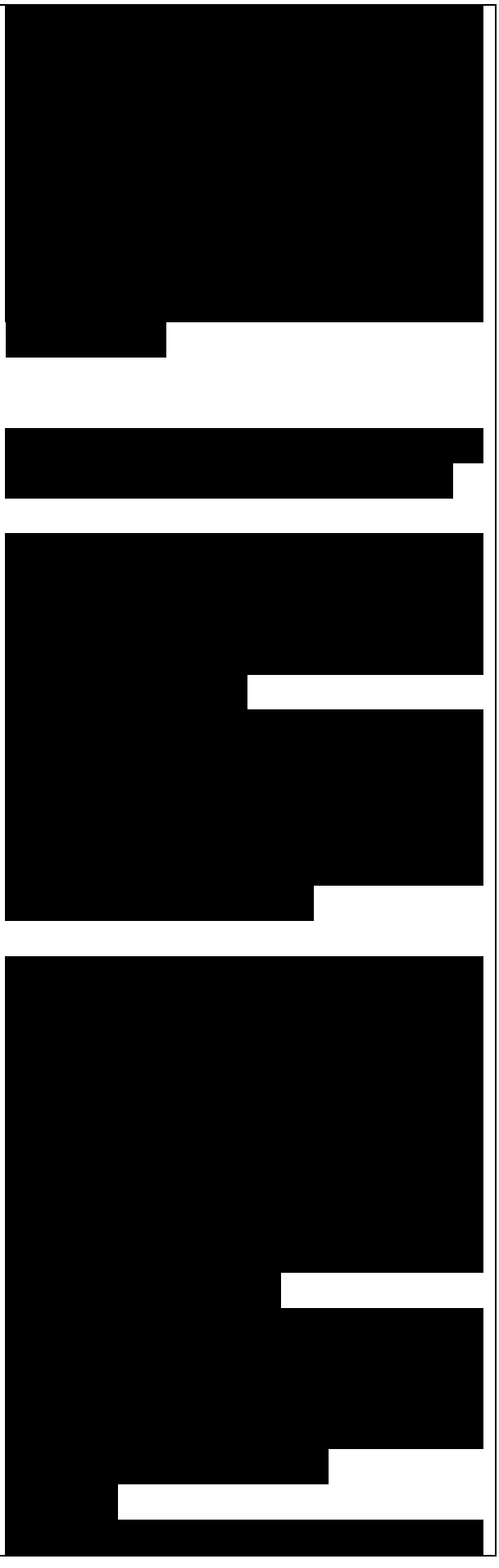

t = number of iterations (generations); vfg = g-th component of velocity of particle j at iteration t, Vgmin < vfg < Vgmax;
J;g g J ;g g w = inertia weight factor; c1, c2 = cognitive and social acceleration factors, respectively; r1, r2 = random numbers uniformly distributed in the range .0; 1/; xj'g = gth component of position of particle j at iteration t; pbestJ = pbest of particle j; and gbestg = gbest of the group.

The j th particle in the swarm is represented by a g-dimensional vector, xj = (xJ;1, xjt2,::., x j ;g), and its rate of position change (velocity) is denoted by another g- dimensional vector, vj = (vj;1 , vj;2 ,..., vj;g/. The best previous position of the j th particle is represented as pbest J = (pbest J^ , pbest j2 ,..., pbest Jg). The index of the best particle among all of the particles in the group is represented by gbestg. In PSO, each particle moves in the search space with a velocity according to its own previous best solution and its group's previous best solution. The velocity update in PSO consists of three parts, namely, momentum, cognitive, and social. The balance among these parts determines the performance of a PSO algorithm. The parameters c1 and c2 determine the relative pull of pbest and gbest, and the parameters r1 and r2 help in stochastically varying these pulls. In the above equations, superscripts denote the iteration number. Figure 4 shows the velocity and position updates of a particle for a two-dimensional parameter space.

5. Results and Discussion

The SimPowerSystems toolbox [14] is

used for all simulations and SSSC-based damping controller design. In a power-system stability study, the fast oscillation modes resulting from the interaction of linear R, L, and C elements and distributed parameter lines are of no interest. These oscillation modes, which are usually located above the fundamental frequency of 50 Hz or 60 Hz, do not interfere with the slow machine modes and regulator

Figure 4. Description of velocity and position updates in PSO technique.

time constants. The phasor solution method is used here, where these fast modes are ignored by replacing the network's differential equations by a set of algebraic equations. The state-space model of the network is replaced by a transfer function that is evaluated at the fundamental frequency and relating inputs (current injected by machines into the network) and outputs (voltages at machine terminals). The phasor solution method uses a reduced state-space model consisting of slow states of machines, turbines, and regulators, thus dramatically reducing the required simulation time. In view of the above, the phasor model of the SSSC is used in the present study.

5.1. Single-machine Infinite-bus Power System with a SSSC

In order to optimally tune the parameters of the SSSC-based damping controller, as well as to assess its performance, a single-machine infinite-bus power system with an SSSC, depicted in Figure 1, is considered in the first instance. The model of the sample power system, shown in Figure 1, is developed using

SimPowerSystems blockset. The system consists of a of 2100-MVA, 13.8-kV, 60-Hz hydraulic generating unit, connected to a 300-km long double-circuit transmission line through a three-phase 13.8/500-kV step-up transformer and a 100-MVA SSSC. All of the relevant parameters are given in Appendix A.

For the purpose of optimization of Eq. (5), routines from the PSO toolbox [19] are used. For the implementation of PSO, several parameters are required to be specified, such as c1 and c2 (cognitive and social acceleration factors, respectively), initial inertia weights, swarm size, and stopping criteria. These parameters should be selected carefully for efficient performance of PSO. The constants c1 and c2 represent the weighting of the stochastic acceleration terms that pull each particle toward pbest and gbest positions. Low values allow particles to roam far from the target regions before being tugged back. On the other hand, high values result in abrupt movement toward, or past, target regions. Hence, the acceleration constants were often set to be 2.0 according to past experiences. Suitable selection of inertia weight, w, provides a balance between global and local explorations, thus requiring less iteration on average to find a sufficiently optimal solution. As originally developed, w often decreases linearly from about 0.9 to 0.4 during a run [17, 18]. One more important point that more or less affects the optimal solution is the range for unknowns. For the very first execution of the program, wider

solution space can be given, and after getting the solution, one can shorten the solution space nearer to the values obtained in the previous iterations.

The objective function is evaluated for each individual by simulating the sample power-system model, considering a severe disturbance. For objective function calculation, a three-phase short-circuit fault in one of the parallel transmission lines is considered. The computational flow chart of the PSO algorithm is shown in Figure 5. While applying PSO, a number of parameters are required to be specified. An appropriate choice of these parameters affects the speed of convergence of the algorithm. Table 1 shows the specified parameters for the PSO algorithm. Optimization is terminated by the prespecified number of generations and was performed with the total number of generations set to 50. The convergence rate of objective function J for gbest with the number of generations is shown in Figure 6. Table 2 shows the optimal values of the SSSC-based controller parameters obtained by the PSO algorithm.

The controller is designed at nominal operating conditions when the system is subjected to one particular severe disturbance (three-phase fault). To show the robustness of the proposed design approach, different operating conditions and contingencies are

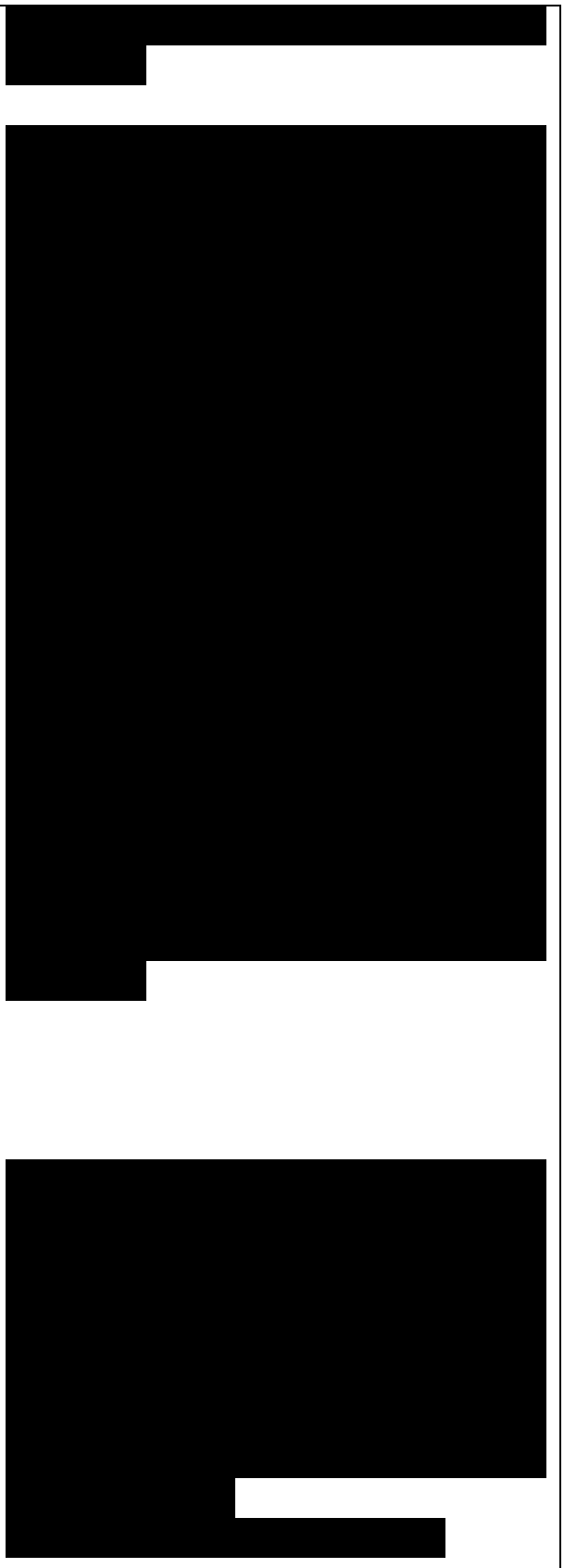

Figure 5. Flow chart of a PSO algorithm.

considered for the system with and without a controller. In all cases, the optimized parameters obtained for the

nominal operating condition, given in Table 2, are used as the controller parameters. Three different operating conditions (nominal, light, and heavy) are considered, and simulation studies are carried out under different fault disturbances and fault-clearing sequences. The response without a controller is shown with dotted lines with the legend "Uncontrolled," and the response with a PSO-optimized SSSC- based damping controller is shown with solid lines with the legend "PSOSSSC."

5.1.1. Case 1: Nominal Loading (Pe = 0.75 p.u., = 45.3°). The behavior of the proposed controller is verified at a nominal loading condition under severe disturbance. A three-cycle, three-phase fault is applied at the middle of one transmission line connecting Bus 2 and Bus 3 at t = 1 sec. The fault is cleared by permanent tripping of the faulted line. The system response under this severe disturbance is shown in Figures 7(a)-7(e), where the plots are the power angle 1 in degrees; the real power flow in the healthy transmission line, PL1, in MW; the generator terminal voltage, VT, in per unit; the speed deviation in p.u.; and the SSSC-injected voltage, Vq, in p.u., respectively. It is clear from these figures that the system is unstable

Table 1
Parameters used for the PSO technique

Swarm size	20
Maximum number of generations	50

Figure 6. Convergence of objective function for gbest.

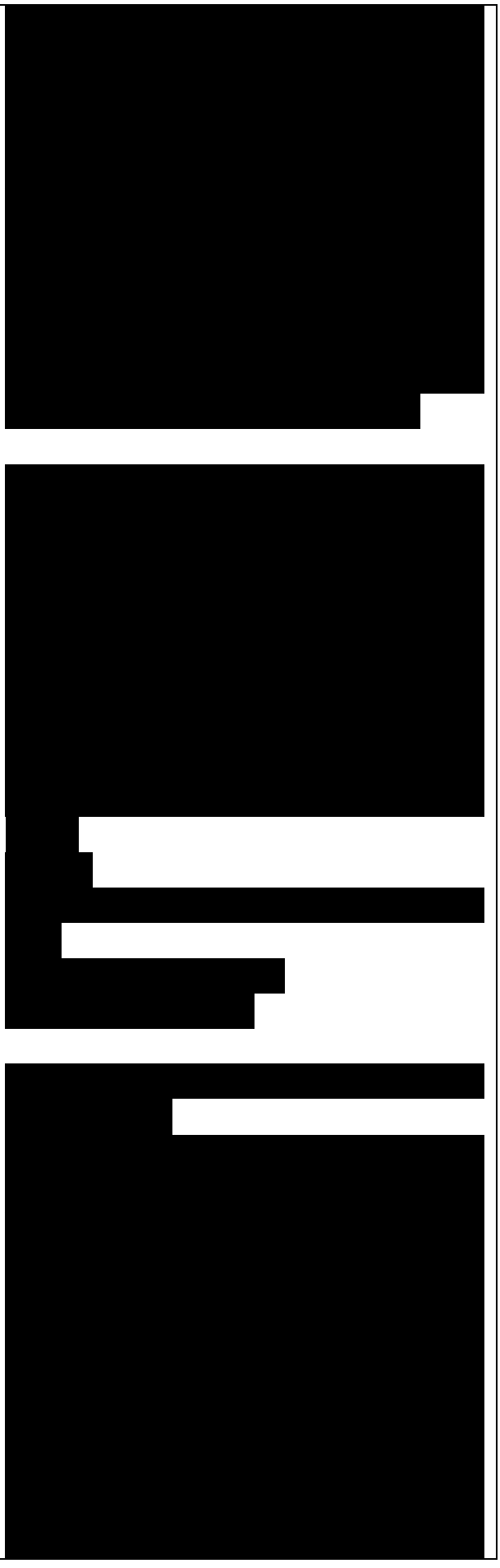

without control under this severe disturbance. Stability of the system is maintained, and the first swing in rotor angle is significantly reduced from 1 = 79.71° (without control) to 1 = 66.27° (with control), with a settling time of 2.9 sec with the application of the proposed SSSC-based controller. It can also be seen that the proposed controller provides good damping characteristics to low-frequency oscillations and quickly stabilizes the system by modulating the SSSC-injected voltage. Hence, the proposed SSSC-based controller extends the power-system stability limit and the power transfer capability. It should be noted here that the proposed controller is designed to improve the stability during the disturbance period. The reactance of the transmission line (x) increases in the post-fault steady-state period because the fault is cleared by permanent tripping of one parallel transmission line. Assuming that the mechanical input power remains constant during the disturbance period, to transmit the same power PL (PL = V1V2 sin 1/x), the power angle (1) increases from 45.3° to 62.2° in the post-fault period.

Another severe disturbance is considered at this loading condition. A three-cycle, three-phase fault is applied at Bus 3 at t = 1 sec, and the fault is cleared by opening both of the lines. One of the lines is reclosed after three cycles, and the other is reclosed after

Table 2
Optimized SSSC-based controller parameters obtained by the PSO technique

SSSC-based controller

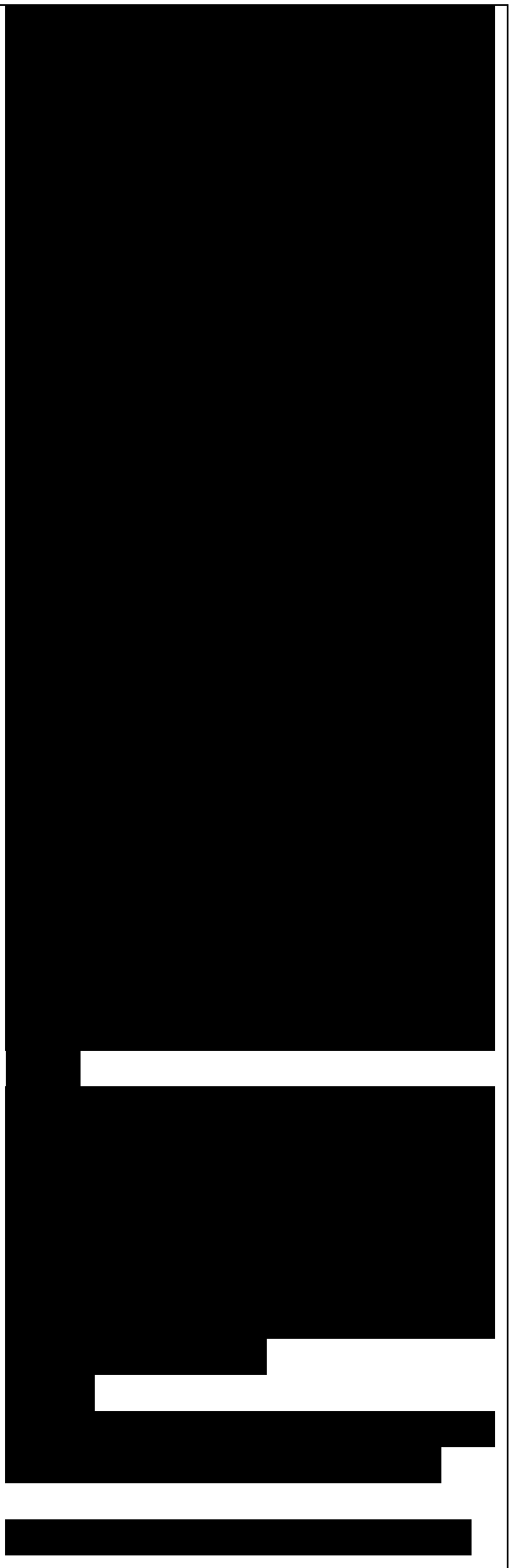

parameters

System/Parameters	KS	Tls	T3S
Single-machine infinite-bus	73.9296	0.2828	0.2765
Three-machine power system	59.4152	0.3292	0.2303

Figure 7. (Continued).

6 sec. The system response to this disturbance is shown in Figures 8(a) and 8(b), where it can be seen that the system loses synchronism for the above contingency. However, with the proposed SSSC controller, the generator remains in synchronism, and power-system oscillations are quickly damped out. It can also be seen from Figure 8(a) that the first swing in rotor angle is reduced from 1 = 97.2° (without control) to 1 = 86.9° (with control) with the application of the proposed SSSC-based controller.

5.1.2. Case 2: Light Loading (Pe = 0.4 p.u., 10 = 22.91°). To test the robustness of the controller to the operating condition and location of the fault, the generator loading is changed to light-loading condition, and a three-cycle, three-phase fault at Bus 1 at t = 1 sec is considered. The original system is restored after fault clearance. The system response under this contingency is shown in Figure 9, which clearly depicts the robustness of the proposed controller for changes in operating condition and fault location. In this case, a reduction in the first swing in the rotor angle from 1 = 25.92° (without control) to 1 = 25.06° (with control) and a settling time of 3.4 sec is achieved with the application of the proposed controller.

Figure 8. System response for a three-cycle, three-phase fault at Bus 3 at

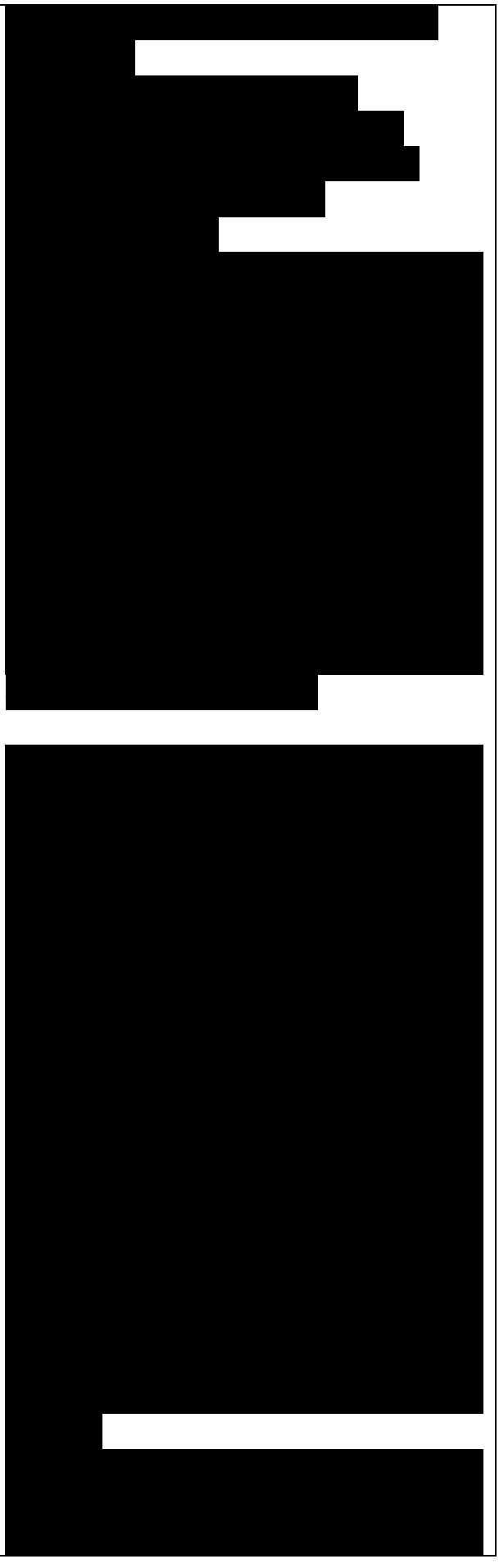

nominal loading followed by both lines tripping: (a) power angle, 1 and (b) SSSC-injected voltage, Vq.

The effectiveness of the proposed controller on unbalanced faults is also examined by applying different types of unsymmetrical faults, namely the double line-to-ground (L- L-G), line-to-line (L-L), and single line-to-ground (L-G) faults, near Bus 3 at t = 1 sec. The duration of each unbalanced fault is assumed to be of three cycles, and the original system is restored after the clearance of the fault. The system response for the above unbalanced contingencies is shown in Figure 10, which also shows the uncontrolled response for the least-severe fault, i.e., single LG fault. It is clear from Figure 10 that, even for the least-severe fault, the power-system oscillations are poorly damped in the uncontrolled case. It is also clear that the proposed SSSC-based damping controller is effective under various unbalanced faults and rapidly stabilizes the power angle in all cases. Comparing the two L-G fault cases (without and with control), it can be seen that the first swing in rotor angle is also reduced slightly from 1 = 23.8° (without control) to 1 = 23.52° (with control) with the application of the proposed SSSC-based controller, and the power angle settles to its initial value at 3.2 sec.

5.1.3. Case 3: Heavy Loading (Pe = 1.0 p.u., 10 = 60.7°). The robustness of the proposed controller is also tested at a heavy-loading condition. Figure 11 shows the

Figure 9. System response for a three-cycle, three-phase fault at Bus 1 at light loading.

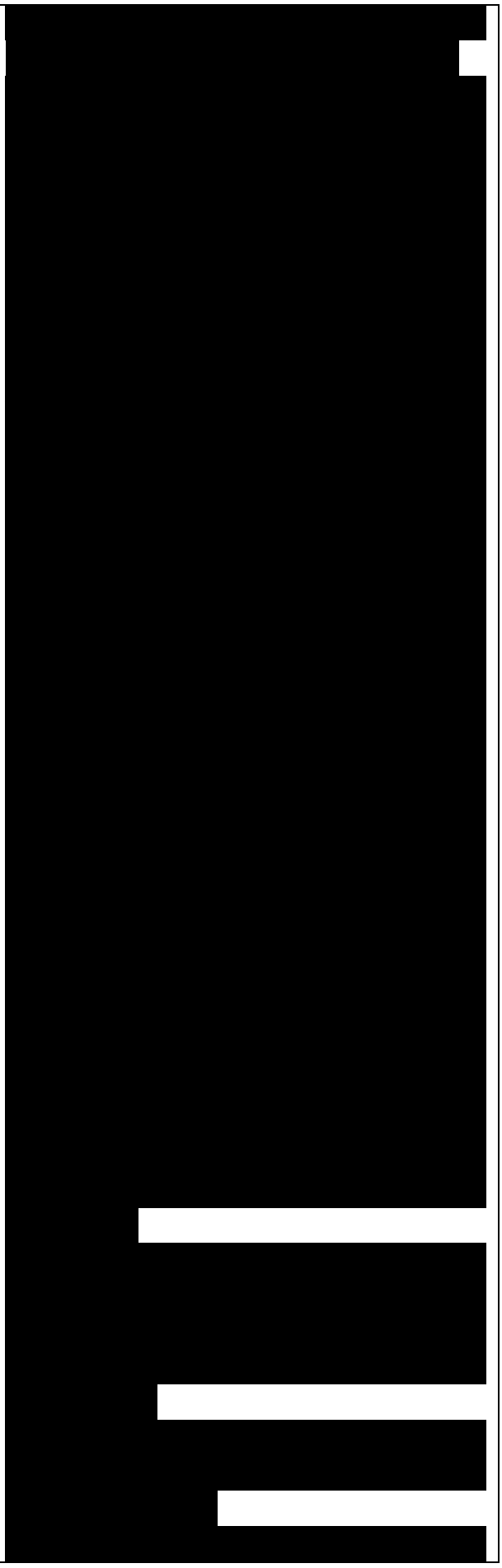

Figure 10. System response for three-cycle unbalanced faults at Bus 1 at light loading.

Figure 11. System response for a three-cycle fault at Bus 3 at heavy loading.

system response for a three-cycle, three-phase fault at Bus 3 at t = 1 sec. The fault is cleared by opening both of the lines, and the lines are reclosed after three cycles. It can be clearly seen from Figure 11 that for the given operating condition and contingency, the system is unstable without control. Stability of the system is maintained, and the first swing in rotor angle is reduced from 1 = 101.2° (without control) to 1 = 97.1° (with control) with a settling time of 3.2 sec with the application the of proposed SSSC-based controller.

5.2. Multi-machine Power System with an SSSC

The proposed approach of designing and optimizing the parameters of an SSSC-based damping controller is also extended to a multi-machine power system, shown in Figure 12. It is similar to the power systems used in [20] and [21]. The system consists of three generators divided into two subsystems and are connected via an intertie. Following a disturbance, the two subsystems swing against each other, resulting in instability. To improve the stability, the line is sectionalized and an SSSC is assumed on the mid-point of the tie-line. The relevant data for the system is given in Appendix A.

Local control signals, although easy to get, may not contain the inter-area oscillation modes. So, compared to wide-area signals, they are not as

highly controllable and observable for the inter-area oscillation modes. Owing to the recent advances in optical fiber communication and global positioning systems, the wide-area measurement system can realize phasor measurement synchronously and deliver it to the control center even in real time, which makes the wide-area signal a good alternative for control input. In view of the above, the speed deviation of generators G1 and G2 is chosen as the control input of the SSSC-based damping controller in this article.

Load flow is performed with Machine 1 as a swing bus and Machines 2 and 3 as PV generation buses. The initial operating conditions used are:

Machine 1 generation: Pe 1 = 3480.6 MW (0.8287 p.u.), Qe 1 = 2577.2 MVAR (0.6136 p.u.)
Machine 2 generation: Pe2 = 1280 MW (0.6095 p.u.), Qe2 = 444.27 MVAR (0.2116 p.u.)
Machine 3 generation: Pe3 = 880 MW (0.419 p.u.), Qe3 = 256.33 MVAR (0.1221 p.u.)

The same approach explained in Section 5.1 for the single-machine case is followed to optimize the SSSC-based damping controller parameters for the three-machine case.

Figure 12. Three-machine power system with an SSSC.

The optimized values of the controller are shown in Table 2. Simulation studies are carried out and presented under different contingencies. The responses of the system when the PSO-optimized SSSC damping

controller is present are shown with solid lines with the legend "PSOSSSC." The uncontrolled response is shown with dotted lines with the legend "Uncontrolled." The following cases are considered.

5.2.1. Case 1. A three-cycle, three-phase fault is applied at one of the line sections between Bus 1 and Bus 6, near Bus 6, at t = 1 sec. The fault is cleared by opening the faulty line, and the line is reclosed after three cycles. The original system is restored after the fault clearance. Figures 13(a)-13(d) show the variations of the inter-area and local mode of oscillation and the SSSC-injected voltage against time. From these figures, it can be seen that the inter-area modes of oscillations are highly oscillatory in the absence of an SSSC-based damping controller, and the proposed controller significantly improves the power-system stability by damping these oscillations. Furthermore, the proposed

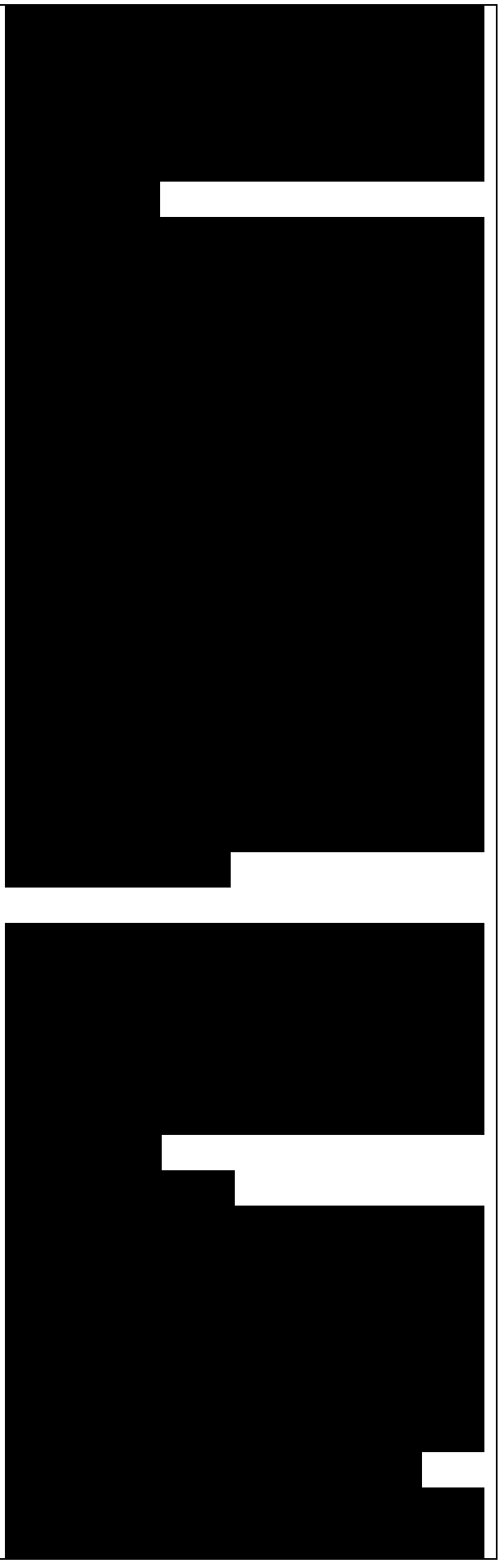

Figure 13. Variation of inter-area and local modes of oscillations against time for a three-cycle, three-phase fault near Bus 6: (a) and (b) inter-area mode; (c) local mode; (d) SSSC-injected voltage, Vq; and (e) SSSC-injected voltage, Vq. (continued)

Figure 13. (Continued).

controller is also effective in suppressing the local mode of oscillations. The power flow through the tie-line (at Bus 1) for the above contingency is shown in Figure 14, which clearly shows the effectiveness of the proposed controller to suppress power-system oscillations.

5.2.2. Case 2. The effectiveness of the

proposed controller on unbalanced faults is also examined by applying self-clearing type unsymmetrical faults, namely L-L-G, L-L, and L-G faults, each of three-cycle duration at Bus 1 at t = 1 sec. The inter-area and local modes of oscillations against time are shown in Figures 15(a) and 15(b). In the figures, the uncontrolled system response for the least-severe single L-G fault is also shown with dotted lines. It is clear from the figures that the power-system oscillations are poorly damped in the uncontrolled case, even for the least-severe L-G fault, and the proposed SSSC-based damping controller effectively stabilizes the power angle under various unbalanced fault conditions.

5.2.3. Case 3. In order to examine the effectiveness of the proposed controller under small disturbance, the load at Bus 4 is disconnected at t = 1 sec for 100 ms. Figures 16(a) and 16(b) show the variations of the inter-area and local modes of oscillations against

Figure 14. Variation of tie-line power flow for a three-cycle, three-phase fault near Bus 6 cleared by a three-cycle line tripping.

Figure 15. Variation of inter-area and local modes of oscillations against time for three-cycle unbalanced faults at Bus 1: (a) inter-area mode and (b) local mode.

Figure 16. Variation of inter-area and local modes of oscillations against time under small disturbance: (a) inter-area mode and (b) local mode.

time, from which it is clear that the proposed SSSC-based damping controller damps the modal oscillations effectively, even for small disturbance.

6. Conclusions

This article presents an SSSC-based damping controller for power-system stability im-provement. For the proposed controller design problem, a non-linear, simulation-based objective function to increase the power-system stability is used, and the PSO technique is employed to optimally tune the parameters of the controller. The effectiveness of the proposed SSSC-based damping controller in improving power-system stability is demonstrated for both single-machine infinite-bus and three-machine power systems. It is observed that the proposed SSSC-based controller provides efficient damping to power-system oscillations and greatly improves the system voltage profile. Further, the proposed controller is found to be robust to fault location and change in operating condition, as it adapts itself to generate a suitable variation of the control signals, depending on the operating condition of the power system. Also, the inter-area and local modes of power- system oscillations are effectively damped by using the proposed SSSC controller.

Appendix A

A complete list of parameters used appears in the default options of SimPowerSystems in the user's manual [14]. All data are in p.u. unless specified otherwise.

Single-machine Infinite-Bus Power System
Generator: SB = 2100 MVA, H = 3.7 sec, VB = 13.8 kV, f = 60 Hz, RS = 2.8544e-3, Xd = 1.305, X'd = 0.296, X" = 0.252, Xq = 0.474, Xq = 0.243, X" = 0.18, Td = 1.01 sec, T'd = 0.053 sec, Tq" = 0.1 sec Load at Bus 2: 250 MW
Transformer: 2100 MVA, 13.8/500 kV, 60 Hz, Ri = R2 = 0.002, L1 = 0, L2 = 0.12, D\/Yg connection, Rm = 500, Lm = 500 Transmission line: 3 Ph, 60 Hz, length = 300 km each, R1 = 0.02546 ^/km, R0 = 0.3864 ^/km, L1 = 0.9337e-3 H/km, L0 = 4.1264e-3 H/km, C1 = 12.74e-9 F/km, C0 = 7.751e-9 F/km
Three-machine Power System
Generators: SB1 = 4200 MVA, SB2 = SB3 = 2100 MVA, H = 3.7 sec, VB = 13.8 kV, f = 60 Hz, RS = 2.8544e—3, Xd = 1.305, Xd = 0.296, X" = 0.252, Xq = 0.474, Xq = 0.243, X" = 0.18, Td = 1.01 sec, T'd = 0.053 sec, Tq" = 0.1 sec Loads: Load 1 = 7500 MW + 1500 MVAR, Load 2 = Load 3 =25 MW, Load 4 = 250 MW
Transformers: SBT1 = 2100 MVA, SBT2 = SBT2 = 2100 MVA, 13.8/500 kV, f = 60 Hz, R1 = R2 = 0.002, L1 = 0, L2 = 0.12, D1/Yg connection, Rm = 500, Lm = 500
Transmission lines: 3-Ph, 60 Hz, line lengths L1 = 175 km, L2 = 50 km, L3 = 100 km, R1 = 0.02546 ^/km, R0 = 0.3864 ^/km, L1 = 0.9337e-3 H/km, L0 = 4.1264e-3 H/km, C1 = 12.74e-9 F/km, C0 = 7.751e-9 F/km HTG: Ka = 3.33, Ta = 0.07, Gmin = 0.01, Gmax = 0.97518, Vg = —0.1 p.u./sec, Vg max = 0.1 p.u./sec, Rp = 0.05, Kp = 1.163, K, = 0.105, Kd = 0, Td = 0.01 sec, P =

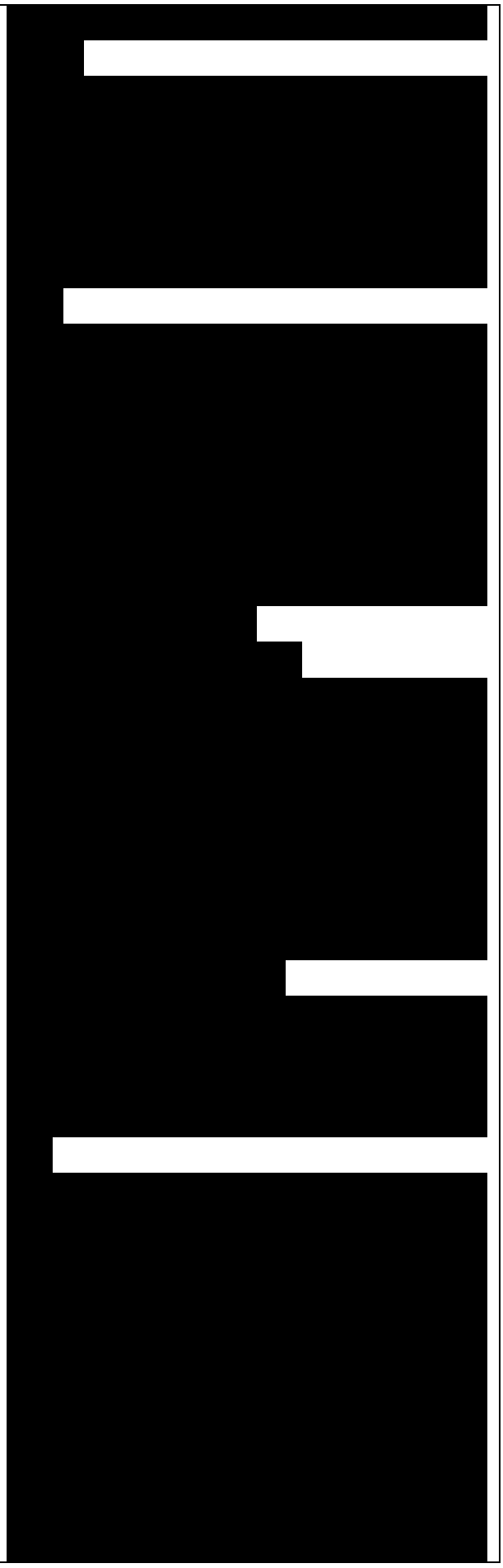

0, Tw = 2.67 sec Excitation system: TLP = 0.02 sec, Ka = 200, Ta = 0.001 sec, Ke = 1, Te = 0, Tb = 0, Tc = 0, Kf = 0.001, Tf = 0.1 sec, Ef min = 0, Ef max = 7, Kp = 0 SSSC: converter rating, Snom = 100 MVA; system nominal voltage, VBom = 500 kV; frequency, f = 60 Hz; maximum rate of change of reference voltage, Vqref = 3 p.u./s; converter impedances, R = 0:00533, L = 0:16; DC-link nominal voltage, VDC = 40 kV; DC-link equivalent capacitance, CDC = 375 x 10“6 F; injected voltage regulator gains, KP = 0.00375, K, = 0.1875; DC voltage regulator gains, KP = 0.1 x 10“3, K, = 20 x 10“3; injected voltage magnitude limit, Vq = ±0.2

Appendix B

For the VSC, two technologies can be used: VSC using GTO-based square-wave multi-level converters and VSC using IGBT-based PWM converters. One phase leg of a three- level converter and PWM converter are shown in Figures A(i) and A(ii), respectively. Each phase of the three-level converter consists of two clamping diodes, four GTO thyristors, and four freewheeling diodes. Each half of the phase leg is split into two series-connected valves, and the mid-point of the valves is connected by diodes to the mid-point, N, of the DC capacitor. By doubling the number of valves with the same voltage rating, the DC voltage doubles and, hence, the power capacity of the converter. In three-level converters, the harmonic components of the output voltage are fewer than those of the conventional two-level converters at the same

switching frequency. In addition, since the blocking voltage of each switching device is less than the DC-link voltage, it is easy to realize high-voltage and large-capacity inverter systems with three-level converters.
In three-level converters, the AC output voltage can be controlled by varying the width of the voltage pulses and/or the amplitude of the DC bus voltage. In PWM converters, the variation in AC voltage is achieved by having multiple pulses per half-cycle and then by varying the width of the pulses. In a PWM-based converter, adequate flexibility of rapid AC voltage control (the AC output voltage can be controlled from zero to maximum) is possible without having to change the DC voltage level by combining the phase-to-neutral and phase-to-phase voltages through separate wye and delta transformers. The control of DC voltage can then be optimized for other considerations. The AC voltage waveform can be chopped in many ways with different control waveforms and numerical programs.

The DC-link voltage and the total capacitance of the DC link are related to the converter rating. The energy stored in the capacitance (in joules), divided by the converter rating (in VA), is a time duration that is usually a fraction of a cycle at nominal frequency.

Figure A. Schematic diagram of a three-level and PWM converter: (i) three-level converter and (ii) PWM converter.